

STUDY THE ORIFICE EFFECTS OF A SYNTHETIC JET ACTUATOR DESIGN

Md Nizam Dahalan*, Shuhaimi Mansor, Muhammad Muzakir Faiz Ali

Aeronautic Laboratory, Faculty of Mechanical Engineering, Universiti Teknologi Malaysia, 81310 UTM Johor Bahru, Johor, Malaysia

Article history

Received

20 July 2015

Received in revised form

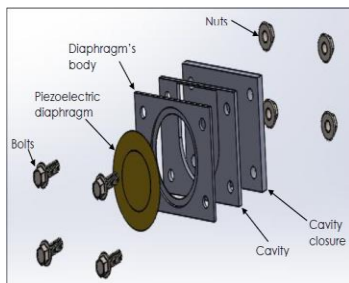
23 September 2015

Accepted

22 October 2015

*Corresponding author
nizam@fkm.utm.my

Graphical abstract



Abstract

The synthetic jet actuator is an active flow control device that is used to improve the aerodynamic performance on working surfaces such as wings, helicopter blades and ground vehicles. The performance of synthetic jet actuator depends on the design of the orifice and cavity, and the oscillating driver. Piezoelectric diaphragm was used as an oscillating driver because of its small size and easier installation. The focus of this project is to study the effects of orifice size and shape for a synthetic jet actuator design. The effects were studied on circular and rectangular shapes, and different sizes of orifice. Meanwhile, the configurations of the cavity are fixed. Experiments were performed to determine the maximum pulse jet velocity and turbulence intensities of the jet coming out of the orifice, driven by the Piezoelectric diaphragm at different frequencies, at constant input voltage of 2V. The experiment mainly involved the measurement of the exit pulse jet velocity using a hot-wire anemometer. The results demonstrated that the circular orifice produced higher maximum pulse jet velocity and smaller sizes orifices, both circular and rectangular, results in higher velocity jets.

Keywords: Synthetic jet actuator, active flow control device, orifice, pulse jet velocity

© 2015 Penerbit UTM Press. All rights reserved

1.0 INTRODUCTION

The aerodynamic performance of the aircrafts, helicopters and road vehicles can be improved by controlling the air flow over the working surfaces, for example wings and rotary blades, especially when operating at high angles of attack. This condition occurs when the boundary layer and the shear flow on the suction surface are manipulated until the separation region is reduced. There are two types of devices in controlling the air flow, which is active and passive flow control. To improve the air flow properties the devices normally were attached to the suitable part of the vehicles. Many flow control devices have been produced and tested by previous researchers to ensure they work as intended [1].

Synthetic jet actuator (SJA) is one of the active flow control device used to control the flow separation on vehicle surfaces, especially on airfoils of aircrafts [1- 4]. In addition, SJA can also be used in the application of heat transfer argumentation [5], vectoring thrusts [6]

and reducing drag in turbulent boundary layers [7]. Basically the design of synthetic jet actuator includes a round or a slot orifice, a cavity and oscillating driver [8]. The pulse air jet was produced through the orifice by oscillating drivers inside the cavity. Four types of oscillating membrane with different drivers which is commonly used to generate synthetic jets are oscillating piston, electromagnetic diaphragm, piezoelectric diaphragm and acoustic excitation.

The selection of piezoelectric diaphragms in this study is due to their small size and, light weight, thus there is no need for external air supply, without complex plumbing, rapid time response, low power consumption and low cost [9]. This type is very suitable to implement in aviation and automotive industry, especially to improve the flow separation on the airfoil of the wing.

The performance of SJA depends on parameters such as orifice, cavity, frequency, voltage, oscillation amplitude and fluid properties [10]. Dahalan [11] in the study of cavity effect found that the smaller size of

cavity volume results in better performance of SJA. Similarly, in a study of the supply voltage effects, it was found that an increase in voltage will increase the maximum pulse jet velocity. However, the power supply unit has a limit of only 2V. Thus the supply is attached to a voltage amplifier of 100 gain to give about 200V to the piezoelectric diaphragm, for each frequency setting [12]. Other studies had also been done on different shapes of the orifice to see its efficiency and to generate the peak jet velocities [13]. The size of the orifice and the natural frequency of the diaphragm play important role in determining the performance of the SJA. Therefore, the objective of this project is to study the effects of orifice based on experiments. The SJA was designed with two different shapes of the orifice and 3 different sizes of each orifice. The experiments were conducted to measure the pulse jet velocity using a hot-wire anemometer at different frequencies with input voltage of 2V.

2.0 SYNTHETIC JET ACTUATOR DESIGN

The SJA was designed to consist of four important parts; cavity and orifice body, diaphragm's body, piezoelectric diaphragm and cavity closure (Figure 1).

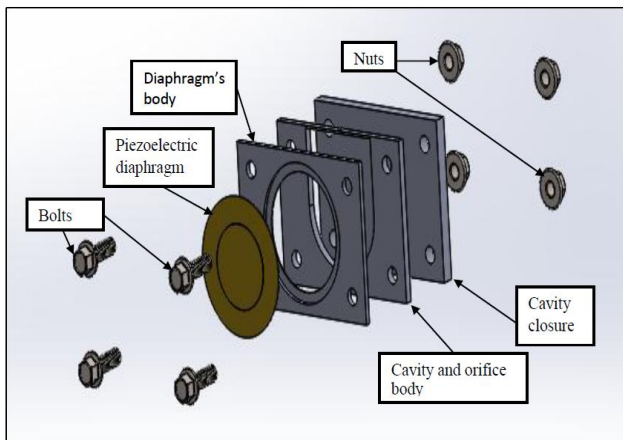


Figure 1 Exploded view of synthetic jet actuator

2.1 Mechanism of Synthetic Actuator.

The most important component of SJA design is the oscillating driver and the piezoelectric diaphragm. The function of the oscillating diaphragm is to generate the air jet pulse through the orifice from the cavity chamber. When the diaphragm oscillates the air from the cavity chamber enters and exits through the orifice. The air from outside, flows into the cavity chamber through the orifice during the injection cycle, as shown in Figure 2 [14].

Then, the air inside the cavity chamber is forced out through the orifice, forming a train of vortex rings. This process is known as the expulsion cycle as shown in Figure 3. The resultant momentum is non-zero although there is no input of mass. Each cycle of the diaphragm

causes a change in the mass of the cavity due to its movement, but the net change in mass is zero and called a zero-net-mass-flux-jet [14].

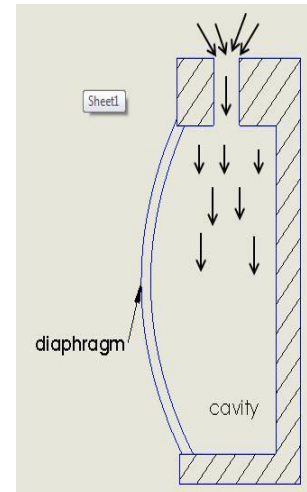


Figure 2 Injection cycle

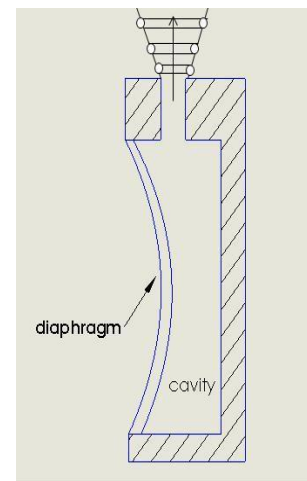


Figure 3 Expulsion cycle

2.2 Estimated Value Formulae

The design of SJA is generally divided into the design of several parameters; operating (amplitude and frequency), geometric (diameter and thickness of the orifice, diameter and height of the cavity) and flow (density and viscosity) [12]. Changing the design specification of SJA can influence the flow characteristic especially the velocity and momentum of the pulse jet. The value of the non-dimensional parameters are indicators of the performance and capabilities of SJA. They are basically, Reynolds number, Re , Stokes number, S , Strouhal number, St , and Helmholtz frequency, f_H . These non-dimensional parameters are used as a guideline in the design of the geometry and estimate the performance of SJA [12-15]. The formula used for the non-dimensional parameters are;

- a) Pulse jet Reynolds number, $R_e = \frac{u_j \times d_o}{\nu}$
- b) Pulse jet Stokes number, $S = \frac{\omega \times d_o^2}{\nu}$
- c) Pulse jet Strouhal number, $St = \frac{S}{R_e} = \frac{f \times d_o}{u_j}$
- d) Helmholtz frequency, $f_H = \frac{c}{2\pi} \sqrt{\frac{A}{L_e V}}$

Where, A = Orifice area, m^2
 c = Speed of sound in air, m/s
 d_o = Orifice diameter, m
 f = Diaphragm's frequency, Hz
 L_e = Effective length of the orifice, m
 V = Cavity volume, m^3
 ν = Fluid kinematic viscosity, m^2/s
 $\omega = 2\pi f$

In order to determine the turbulence intensity, the formulas are as follows [16]:

- i. Mean velocity = $\frac{1}{N} (\sum_i^N U_i)$
- ii. Root mean square velocity, $U_{RMS} = \sqrt{\frac{1}{N} \sum_{i=1}^N (U_i')^2}$
- iii. Turbulence intensity = $\frac{U_{RMS}}{\text{Mean velocity}} \times 100$

where, U_i = Discrete velocity at t time

$U_i' = U_i - \text{Mean Velocity}$

N = Number of data

3.0 EXPERIMENTAL SETUP

3.1 Fabrication

The fabrication process of SJA needs to be done neatly and precisely. A slightly inaccuracy, defects and misalignment on SJA model can influence the air pulse jet produced. The fabrication of SJA mainly used wire cut machine and milling machine. Wire cut machine was used to fabricate the crucial part of SJA especially for rectangular orifice and cavity hole.

3.2 Configurations of SJA

This project focused on the effects of the orifice of SJA. Two different shapes (circular and rectangular) with three different sizes for each orifice shape were designed and manufactured. Meanwhile, the configurations of the cavity were fixed, using the curved shaped cavity with thickness of 4mm giving the cavity volume of $4.923 \times 10^{-6} m^3$. Table 1 shows the specifications of circular orifice and Figure 4 shows the isometric drawing of SJA cavity body with circular orifice.

Table 1 Specifications of circular shaped orifice

	Size A	Size B	Size C
Diameter, d_o (mm)	1	1.5	2
Area, A (mm^2)	0.785	1.767	3.14

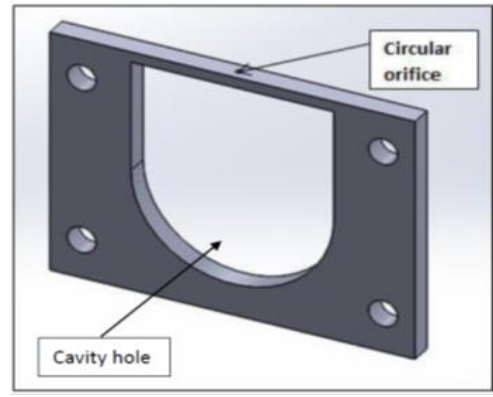


Figure 4 Cavity body with circular orifice

Table 2 shows the specification of rectangular orifice sizes and Figure 5 is an isometric drawing of SJA cavity body with rectangular orifice.

Table 2 Specifications of rectangular shaped orifice

	Size A	Size B	Size C
Diameter, d_o (mm)	2	2	2
Length, l (mm)	6	8	10
Area, A (mm^2)	12	16	20

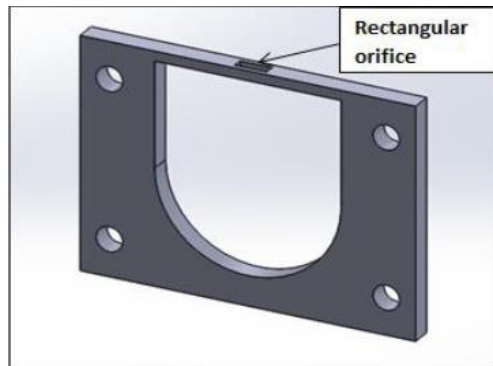


Figure 5 Cavity body with rectangular orifice

3.3 Experimental Equipment and Measurement

The experimental schematic is shown in Figure 6. Power supply or function generator was used to supply the voltage and frequency signals to power the piezoelectric diaphragm. The testing involves manipulating the applied frequencies and input voltages of the SJA under a square waveform. The function generator can supply the voltage in the range of 10 mVp-p to 10 Vpp and frequency up to 12.5 MHz. However, the input voltage was set to a constant throughout the experiment which is 2 Vp-p and the applied frequency is set from 100 Hz to 1000 Hz with the increments of 100 Hz. The SJA needs high voltage to vibrate the piezoelectric diaphragm then to produce better pulse jet velocity. Then, the Trek Model 601 C two-channel amplifier was used for the

experiment with capabilities to gain the input voltage to 100 times. The SJA produced air pulse jet through the orifice and the velocity was measured using a hot-wire anemometer located 1mm above the centreline of the orifice.

The raw data that was generated from the hot-wire anemometer was filtered using a Data Acquisition System and sent to a computer to be analyzed via a Dantec Dynamic Software called Stream-ware. The applied frequency were varied but the voltage was fixed at 2Vpp. The program was used to analyze all the raw data. The software display shows the pulse jet velocity time trace produced from the orifice of the SJA and also calculated the mean velocity, root mean square velocity and turbulence intensity.

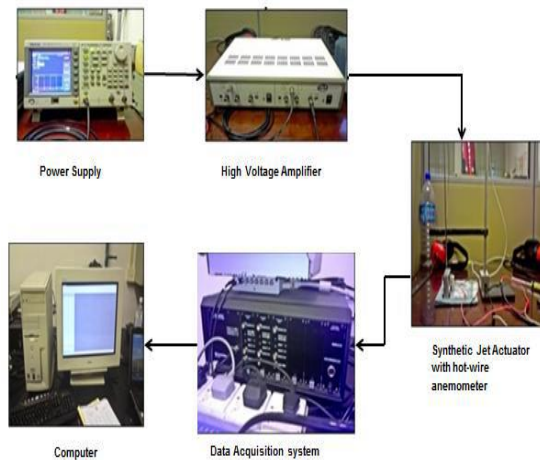


Figure 6 Experimental schematic of synthetic jet actuator

3.4 Calibration of Hot-Wire Anemometer.

The hot-wire anemometer was calibrated using UTM-LST wind tunnel and the velocity in meters per second can be read directly through the computer via Stream-ware program, which is run based on LabView software. The total uncertainty of the hot-wire measurements is between 2.2 and 4.2 percent of the measured velocity. This was calculated according to Santo [17].

4.0 RESULT & DISCUSSION

The objective of this project is to study the effect of the orifice of SJA based on experiments. Two different shapes of orifices (circular and rectangular) of three different sizes for each, were designed, fabricated and tested. The configurations for the cavity and piezoelectric diaphragm were unchanged. The experiments were mainly oriented to measure the pulse jet velocity created by the SJA through the orifice, using a hot wire anemometer. The data was recorded using the Dantec Dynamic Software for 5 seconds with a sampling rate of 1000 Hz. The parameters obtained from these experiments were the

maximum pulse jet velocity, mean velocity, root mean square velocity and turbulence intensity. The mean and root mean square velocities were then used to determine the percentage of turbulence intensity of the jet.

Figure 7 shows a 0.02 s sample of the time trace of the pulsed SJA velocity for the different sizes of circular orifice. The applied frequency of the driving diaphragm was varied, but the input voltage was kept constant at 2 V. The graphs shows that the air velocities can be classified as pulsed jet, which peaked at a given time interval. It was found that the graphs give different values of maximum pulse jet velocities for SJA of different orifice sizes. However, different applied frequencies also affect the pulse jet. Therefore, testing should be done on a range of different frequencies to understand the jet behaviour better, and to determine the maximum pulse jet velocity for each design.

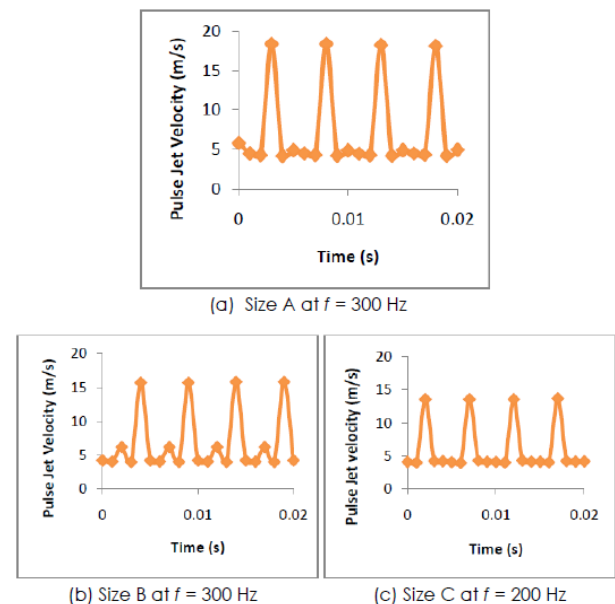


Figure 7 Pulsed Jet velocity time trace of SJA of circular orifice at different applied frequencies, but constant input voltage of 2 V.

Figure 8 presents the experimental data of maximum pulse jet velocity against the applied frequency for different circular sizes of orifice. There were three different sizes of the circular shaped orifice; Size A (0.785 mm^2), size B (1.767 mm^2) and size C (3.142 mm^2). The findings show that the Circular Sized A orifice produced the highest maximum pulse jet velocities that is 20.69 m/s, at the applied frequency of 900Hz compared to Circular Sized B that produced maximum pulse jet velocity of 18.40 m/s at applied frequency of 500 Hz and 600 Hz, while Circular Sized C orifice produced 16.83 m/s at applied frequency of 400 Hz. This shows that the smaller sized orifice would give higher maximum pulse jet velocities. It should be noted that the ability of SJA to produce maximum pulse jet velocity also depended on the frequency. The result

appeared that the SJA of a specific size had performed well with a specific operational frequency.

Figure 9 illustrates the effect of circular orifice area on the best maximum pulse jet velocity. Further analysis showed that the reduction in the size or area of the circular orifice would increase the maximum pulse jet velocity produced.

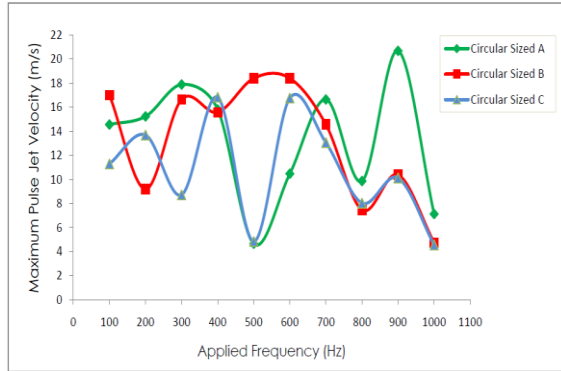


Figure 8 The maximum pulse jet velocity against applied frequency for different circular sized orifice

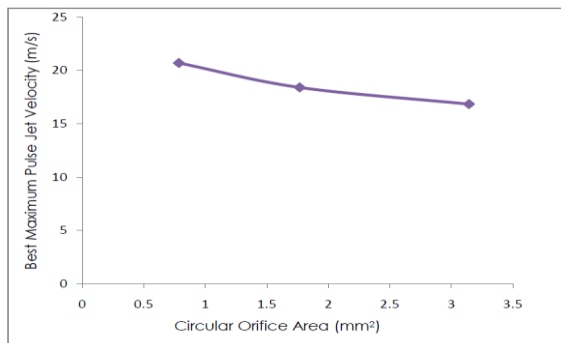


Figure 9 Effect of circular orifice area on the best maximum pulse jet velocity

Figure 10 shows the graph of maximum pulse jet velocity against applied frequency for rectangular shaped orifices of different sizes: Rectangular Size A (12 mm^2), Rectangular Size B (16 mm^2) and Rectangular Size C (20 mm^2). Figure 10 shows that the Rectangular Sized A orifice produced the highest maximum pulse jet velocity, which is 6.67 m/s followed

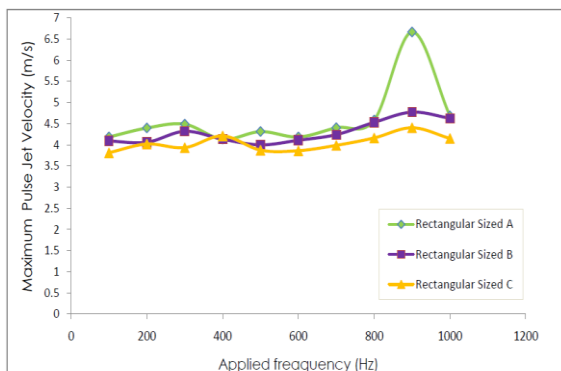


Figure 10 The maximum pulse jet velocity against applied frequency for different rectangular sized orifice

by Rectangular Sized B orifice which produced a jet of velocity 4.73 m/s and Rectangular Sized C produced 4.40 m/s at the same applied frequency of 900 Hz.

Figure 11 shows the effects of rectangle orifice size, at different frequency but constant supply voltage. The result showed similar trend to Figure 9, where reducing the area of rectangular orifice will increase the best maximum pulse jet velocity. These results are in agreement with [18], whose findings showed the effects of width of the slot (rectangular) orifice on maximum ejected velocity. The reduction of the slot width would give better maximum ejected velocity.

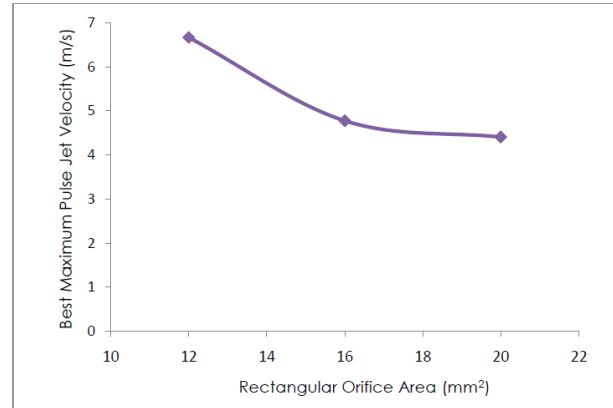


Figure 11 The effects of rectangular orifice area on the best maximum pulse jet velocity

However, the comparison between circular orifice and rectangular orifice shows that circular orifice produces higher maximum pulse jet velocities compared to rectangular orifice. This is because the circular orifice models have smaller size orifices compared to the rectangular orifice models. It was quite difficult to fabricate rectangular orifices to have small sizes comparable to the circular orifices. The rectangular orifice was fabricated using a wire-cut machine, capable of cutting a minimum slot size of 2 mm. To cut a narrower slot would not guarantee dimensional accuracy.

Figures 12 shows the jet turbulence intensity variations with respect to applied vibration frequencies of the diaphragm of the SJA for circular orifice. The graphs do not show specific trends. Figure 13 shows the turbulence intensity variations with respect to applied frequency for rectangular orifice. The figure clearly shows that at 900 Hz, the turbulence intensity rose sharply to maximums of 10.2% for size A, 4.5% for size B and about 3% for size C.

For flow control applications high turbulent intensity jets are required. The SJA needs to produce high turbulence intensity jets to be able to induce enough energy into the main flow so as to prevent separation, especially in turbulent separated flows.

As the size of the orifice increases the natural frequency of the jet would decrease. This condition was also stated in Helmholtz resonance theory. This proved that the performance of SJA would improve if the size of the orifice is reduced.

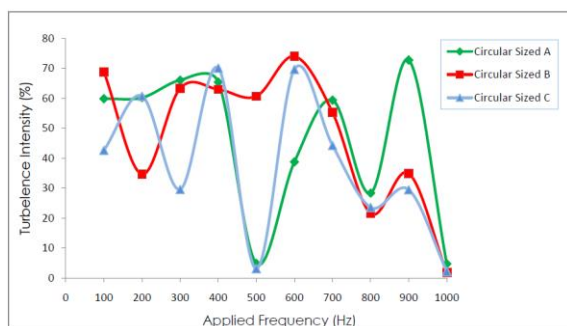


Figure 12 Turbulence intensity variations against the applied frequency for different circular sized orifice

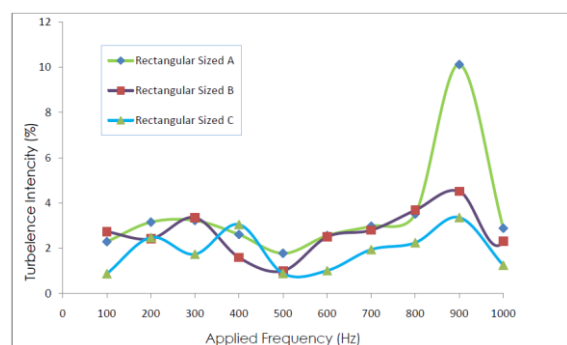


Figure 13 Turbulence intensity variations against the applied frequency for different rectangular sized orifice.

5.0 CONCLUSION

The orifice design effects on a synthetic jet actuator (SJA) driven by a piezoelectric diaphragm were investigated via experimental method. This study focused on two orifice designs of circular and rectangular shapes, each with 3 different sizes. Experiments were conducted to measure the pulse jet velocity out of the orifices using a hot-wire anemometer. The diaphragm was driven at different frequencies but with constant input voltage of 2 V.

The experimental results showed that the ability of SJA to produce maximum pulse jet velocity depends on the applied frequency and the orifice size, while other parameters were unchanged, namely the diaphragm, and the chamber volume and shape. Each orifice shape has its own optimum applied frequency that gives optimum SJA performance. This study has also found that generally the maximum pulse jet velocity and percentage of turbulence intensities increases if the size of the orifice is reduced. This is true for both shapes of the orifice; circular and rectangular.

The findings of this investigation complemented those of earlier studies. In addition, these findings have significant implications for the understanding of how to improve the SJA performance especially for flow separation control applications. However, further experimental investigations are needed to study the effects of orifice depth and the selection of piezoelectric diaphragm of different materials and sizes.

Acknowledgement

The authors would like to express their deepest gratitude to Universiti Teknologi Malaysia (UTM) for providing research grants under the Research University Grant (GUP) scheme (QJ130000.7124.01J42). In addition, the authors thank the UTM Aeronautical Laboratory (UTM Aerolab) for providing the space and equipment needed for this research.

References

- [1] Tuck, A. and Soria, J. 2004. Active Flow Control over a NACA 0015 Airfoil using a ZNMF Jet. *15th Australasian Fluid Mechanics Conference*. Sydney, Australia. 13-17 December 2004. 13-17.
- [2] Seifert, A., Darabi, A. and Wygnanski, I. 1996. Delay of Airfoil Stall by Periodic Excitation. *AIAA Journal of Aircraft*. 33(4): 691-698.
- [3] Gilarranz, J. and Rediniotis, O. 2001. Compact, High- Power Synthetic Jet Actuators for Flow Separation Control. *AIAA*. 2001-0737.
- [4] Kevin, B., Philip and Rhett, J. 2003. Flow Control of a NACA 0015 Airfoil Using a Chord-wise Array of Synthetic Jets. *AIAA*. 2003-0061.
- [5] Guarino, J. R., and Manno, V. P. 2002. Characterization of Laminar Jet Impingement Cooling in Portable Computer Applications. *Components and Packaging Technologies*, IEEE Transactions on. 25(3): 337-346.
- [6] Smith, B. and Glezer, A. 1997. Vectoring and Small Scale Motions Effectuated in Free Shear Flows using Synthetic Jet Actuators. *AIAA*. 97-0213.
- [7] Lee, C.Y. and Goldstein, D.B. 2001. DNS of Microjets for Turbulent Boundary Layer Control. *AIAA*. 2001-1013.
- [8] Holman, R., Uffurkar, Y., Mittal, R., Smith, B.L. and Cattafesta, L. 2005. Formation Criterion for Synthetic Jets. *AIAA Journal*. 43(10): 2110-2116.
- [9] Ugrina, S. 2007. *Experimental Analysis and Analytical Modelling of Synthetic Jet Cross Flow Interactions*. PhD Thesis. Department of Aerospace Engineering, University of Maryland.
- [10] Mittal, R. and Rampunggoon, P. 2001. Interaction of a Synthetic Jet with a Flat Plate Boundary Layer. *AIAA Paper*. 2001-2773.
- [11] Dahalan, M.N., Mansor, S. and Ali, A. 2012. Cavity Effect of Synthetic Jet Actuators Based on Piezoelectric Diaphragm, *Applied Mechanics and Materials*. 225: 85-90.
- [12] Dahalan, M.N., Mansor, S., Shaharudin, M.H. and Ali, A. 2012. Evaluation of Synthetic Jet Actuators Design Performance, *Aircraft Engineering and Aerospace Technology: An International Journal*. 84(6): 390-397.
- [13] Oren, L., Gutmark, E., Muragappan, S. and Khosla, S. 2009. Flow Characteristics of Non Circular Synthetic Jet. *AIAA*. 2009-1309.
- [14] Gomes, L. D., Crowther, W. J., and Wood, N. J. 2006. Towards a Practical Piezoceramic Diaphragm Based Synthetic Jet Actuator for High Subsonic Applications-Effect of Chamber and Orifice Depth on Actuator Peak Velocity. *3rd AIAA Flow Control Conference*. San Francisco, California. 5- 8 June 2006. 5(8): 267-283).
- [15] Zulkafli, N.F. 2010. *Design and Fabrication of Synthetic Jet Actuator*. Bachelor of Engineering Thesis. Universiti Teknologi Malaysia, Skudai, Johor.
- [16] Mohd Shaharudin, M.H. 2011. Performance Evaluation of Synthetic Jet Actuator. *Bachelor of Engineering Thesis*. Universiti Teknologi Malaysia, Skudai, Johor.
- [17] Santos, L.A., Reis, M.L., Mello, O.A. and Mezzalana, L.G. 2006. Propagation of Uncertainties in the Calibration Curve Fitting of Single Normal Hot-wire Anemometry Probes. *XVIII IMEKO*

World Congress, Metrology for a Sustainable Development.
Rio de Janeiro, Brazil. 17–22 September 2006. 17-22

[18] Yang, A.S. 2009. Design Analysis of a Piezoelectrically Driven Synthetic Jet Actuator. *Journal of Smart Materials and Structures*. 18(12): 125004